European Cells and Materials Vol. 10. 2005 (pages 51-60) DOI: 10.22203/eCM.v010a06 ISSN 1473-2262

FOURIER TRANSFORM INFRARED IMAGING OF FOCAL LESIONS IN HUMAN OSTEOARTHRITIC CARTILAGE

E. David-Vaudey[1,2], A. Burghardt[1], K. Keshari[1], A. Brouchet[3], M. Ries[4] and S. Majumdar[1*]

[1]Musculoskeletal and Quantitative Imaging Research Group, Department of Radiology, and [4]Department of Orthopedic Surgery University of California San Francisco, San Francisco, CA, USA
[2]Department of Rheumatology, and [3]Department of Pathology, Hospital Rangueil, University of Paul Sabatier Toulouse, Toulouse, France

Abstract

Fourier Transform Infrared Imaging (FTIRI) is a new method for quantitatively assessing the spatial-chemical composition of complex materials. This technique has been applied to examine the feasibility of measuring changes in the composition and distribution of collagen and proteoglycan macromolecules in human osteoarthritic cartilage. Human cartilage was acquired post-operatively from total joint replacement patients. Samples were taken at the site of a focal lesion, adjacent to the lesion, and from relatively healthy cartilage away from the lesion. Sections were prepared for FTIRI and histochemical grading. FTIRI spectral images were acquired for the superficial, intermediate, and deep layers for each sample. Euclidean distance mapping and quantitative partial least squares analysis (PLS) were performed using reference spectra for type-II collagen and chondroitin 6-sulphate (CS6). FTIRI results were correlated to the histology-based Mankin scoring system. PLS analysis found relatively low relative concentrations of collagen (38 ± 10%) and proteoglycan (22 ± 9%) in osteoarthritic cartilage. Focal lesions were generally found to contain less CS6 compared to cartilage tissue adjacent to the lesion. Loss of proteoglycan content was well correlated to histological Mankin scores ($r=0.69$, $p<0.0008$). The evaluation of biological tissues with FTIRI can provide unique quantitative information on how disease can affect biochemical distribution and composition. This study has demonstrated that FTIRI is useful in quantitatively assessing pathology-related changes in the composition and distribution of primary macromolecular components of human osteoarthritic cartilage.

Keywords: Fourier transform infrared imaging, osteoarthritis, cartilage, collagen, proteoglycan

Abbreviations: CS6 (chondroitin 6-sulphate), FTIRI (Fourier Transform Inrared Imaging), ITM (inter-territorial matrix), OA (osteoarthritis), PLS (Partial Least Squares), TM (territorial matrix)

*Address for correspondence:
Sharmila Majumdar,
Department of Radiology,
University of California, San Francisco
185 Berry St Suite 350
San Francisco, CA 94107

Tel: 415 353-4534
Fax: 415 353-3438
Email: sharmila.majumdar@radiology.ucsf.edu

Introduction

Fourier transform infrared spectroscopy (FTIR) has found applications in industrial purity assessment studies, pharmacological studies, forensic science, and other fields (Ma *et al*., 2001; Realini *et al*., 2001). Additionally it has been used extensively to evaluate protein structure, lipid, and inorganic compounds in tissues (Cooper and Knutson, 1995; Jackson and Mantsch, 1995; Kidder *et al*., 1997). Recently, the coupling of an FTIR spectrometer with an infrared microscope and focal plane array detector (64 x 64 elements) has made it possible simultaneously to obtain 4096 spectra in a spatially discrete manner yielding wavenumber-wise image maps of infrared absorption. While conventional methods such as standard histological techniques, fluorescent probes and stains are useful to display the spatial distribution of cellular and some biochemical components in tissue, quantification with these methods is difficult. Biochemical assays, while quantitative, do not provide information on the spatial distribution of tissue chemistry. Thus, FTIR spectral imaging (FTIRI) is a promising tool for studying tissue biochemistry in both a spatial and quantitative manner.
Pathological tissues that are studied using FTIR and FTIRI cover a wide range of types. These range from white matter in multiple sclerosis, Alzheimer's disease plaque (Choo *et al*., 1996), cancerous tissues (breast, colon, cervical, sarcomas and skin) (Lasch and Naumann, 1998; Gao *et al*., 1999), diseased arteries, silicone or polyester implants of the breast (Kidder *et al*., 1997) to skeletal tissues such as bone and cartilage (Paschalis *et al*., 1997; Boskey *et al*., 1998; Cassella *et al*., 2000). Recent studies have focused on bone mineral content and the organic phase in normal and osteoporotic human bone, in osteogenesis imperfecta (Camacho *et al*., 1996; Cassella *et al*., 2000) and X-linked hypophosphatemia using mice models (Camacho *et al*., 1995). In addition, FTIR provides insight into the function of osteocalcin (Boskey *et al*., 1998) and osteopontin (Boskey *et al*., 2002) on mineralization in a knock-out mouse model as well as the role of collagen in defining mineral properties (Paschalis *et al*., 1996). A few studies have investigated the composition of articular cartilage (Camacho *et al*., 2001; Potter *et al*., 2001) which is of interest in diseases such as osteoarthritis, rheumatoid arthritis and in tissue engineering.

Cartilage is composed of collagen fibrils embedded within a hydrated, proteoglycan gel matrix which expands to maintain stiffness during compression. As the extracellular matrix degrades over time, morphological and chemical changes occur causing the cartilage to

fibrillate and ultimately degrade. Molecular level changes include the fibrillation of the superficial collagen fibres, a disruption of the collagen fibre orientation, and a decrease in proteoglycan (specifically chondroitin and keratan sulphate) and water content. In addition, changes in the amount of other proteoglycans such as biglycan, decorin and aggrecan may be important.

Camacho *et al*. show that FTIRI (Camacho *et al*., 2001) in bovine articular cartilage provides a novel alternative for visualizing cartilage components and clearly depicts the zonal variations in composition, with differences between the superficial, intermediate and deep zones. Using FTIRI coupled with multivariate data processing techniques, Potter *et al*. show that this technique can be used to obtain spatially resolved quantitative compositional data for selected pure components of cartilage i.e. chondroitin 6-sulphate (CS6) and type-II collagen (Potter *et al*., 2001).

In this paper, these ideas have been extended and applied to human osteoarthritic articular cartilage to assess spatial chemical modifications within the different zonal layers at different degrees of degeneration. The zonal distribution of type-II collagen and proteoglycans such as CS6, chondroitin 4-sulphate, aggrecan, biglycan, and decorin has been evaluated in diseased and healthy cartilage. Correlations between histological severity (based on an aggregate Mankin's score and loss of CS6 and type-II collagen have been calculated for the superficial, intermediate, and deep layers. Regions comprising a focal lesion were compared to an adjacent region as well as a distant control region. Additionally, the distribution of collagen in the interterritorial matrix was compared to the territorial matrix surrounding the chondrocytes.

Materials and Methods

Human cartilage specimens

Fresh human cartilage specimens were obtained from patients following joint replacement surgery (knee n=4, hip n=1) in concordance with the Biosafety Committee at the University of California, San Francisco. All subjects underwent surgery for degenerative joint disease (osteonecrotic patients were excluded based on clinical and/or radiological findings). Disease extent was established by pre-operative radiography graded using the Kellgren/Lawrence score (Kellgren and Lawrence, 1957). Within each surgical tissue specimen three samples were identified and extracted with a 6mm dermal punch: (1) A focal lesion, in the tibial compartment with enough cartilage to analyze (for specimens with complete narrowing of the medial compartment, the lateral tibial compartment was used) (2) an adjacent region within 15 mm of the focal lesion, and (3) a control region with no evident degeneration, either the homolateral femoral condyle or in the contralateral side of the tibia when it was possible. Subchondral bone was removed with a scalpel before the cartilage samples were flash frozen in Optimal Cutting Temperature (OCT) compound (Tissue-Tek, Sakura, Tokyo, Japan) and then stored at -80º. Sections with a 7µm thickness were cut perpendicular to the articular surface using a cryostat (CM 1850, Leica Microsystems, Bannockburn, IL). Adjacent sections were transferred to a Barium Fluoride (BaF_2) window for FTIRI and a standard glass slide for histological grading. The OCT embedding material was removed from the FTIRI samples by adding a few drops of de-ionized water and rapid removal with a pipette prior to air-drying the sample. Histological samples were fixed in neutral buffered formalin and stained with Safranin-O (Hyllested *et al*., 2002) and all specimens were evaluated histologically for OA severity.

Histological samples were graded by two trained observers (A. Brouchet and E. David-Vaudey) using a modified Mankin score (Mankin *et al*., 1981), i.e. without scoring the cartilage bone interface (tidemark) and the subchondral bone, as our samples had the bone removed prior to sectioning. The mean score between observers was considered for correlative analyses with the FTIR results.

FTIRI acquisition

FTIRI spectral images were recorded in transmission mode with a commercially available IR imaging system consisting of a mid-infrared step-scan interferometer coupled to an IR microscope that includes a 64 x 64 mercury cadmium telluride focal-plane array detector (ImageMax, Thermo Electron Corporation, Waltham, MA). Each detector element records an interferogram that was averaged over 32 acquisitions. The interferograms were then apodized and Fourier transformed into 16cm^{-1} resolution spectra over the range of 500-4000cm^{-1} for a total of 4096 spectra with a 400µm x 400µm field of view. To investigate regional depth-wise variations in collagen and proteoglycan composition, three acquisitions were made for each sample to cover the superficial, intermediate, and deep layers of cartilage. The three layers were identified histologically based on cell shape. Representative tissue spectra and histology images are shown in Figure 1.

Pure components

FTIR spectra for common components of the extracellular matrix of cartilage were acquired for use in multivariate analyses of the spectral image data described above. Specifically the following components were used: type-II collagen from bovine nasal cartilage; chondroitin 6-sulphate from shark cartilage; chondroitin 4-sulphate from bovine trachea; biglycan, decorin, and aggrecan from bovine articular cartilage (Sigma Aldrich, St. Louis, MO). Each pure component sample was mixed in a potassium bromide matrix (1:100 sample:KBr ratio) and pressed into 7mm pellets. Reference spectra were acquired with the bench interferometer component of the FTIRI system described above (Nexus 870, Thermo Electron Corporation, Waltham, MA). For each component, FTIR spectra with a resolution of 16cm^{-1} were recorded and averaged over 256 acquisitions.

Multivariate Analysis

The cartilage spectral image data were analyzed in a

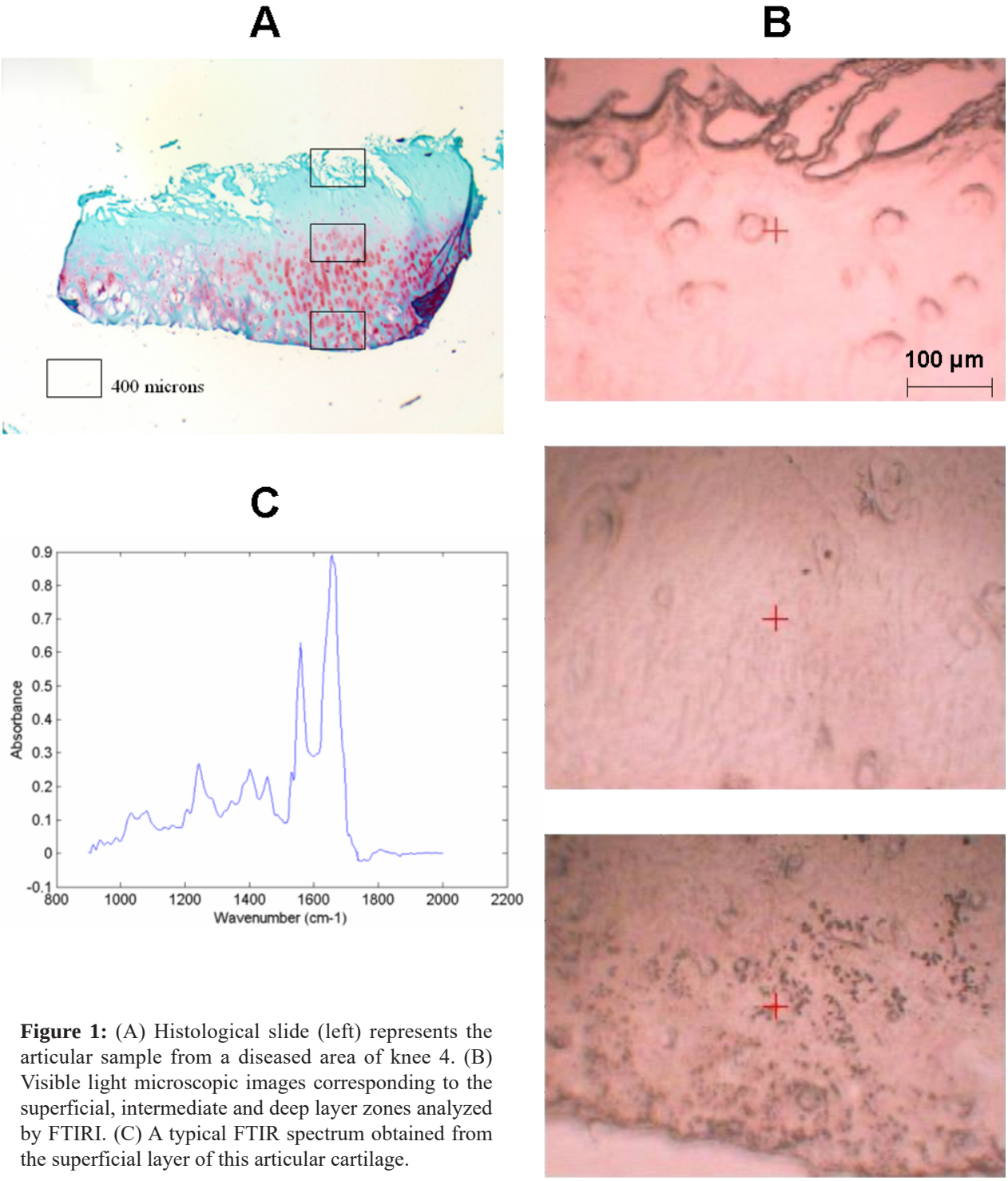

Figure 1: (A) Histological slide (left) represents the articular sample from a diseased area of knee 4. (B) Visible light microscopic images corresponding to the superficial, intermediate and deep layer zones analyzed by FTIRI. (C) A typical FTIR spectrum obtained from the superficial layer of this articular cartilage.

commercial chemical imaging software suite (Isys, Spectral Dimensions, Olney, MD). All Image and reference spectra were truncated to the fingerprint region (900-2000 cm^{-1}) and corrected with a first order baseline subtraction.

The Euclidean distance and partial least squares (PLS) methods described by Potter *et al* (Potter *et al*., 2001) were applied here to examine the distribution of collagen and proteoglycan components in the different cartilage layers and at different degrees of degeneration. The Euclidean distance was calculated between each sample spectral image and a component's reference spectrum on a pixel by pixel basis,

$$D(x,y) = \sqrt{\sum_{i=w_1}^{i=w_2} \left[\tilde{A}(x,y)_i - \tilde{a}_i\right]^2}$$

where $D(x,y)$ is the distance at a point x,y of the spectral image, $\tilde{A}(x,y)_i$ is the vector normalized absorbance at pixel x,y for wavenumber i, $\tilde{a}_i$ is the vector normalized pure component reference absorbance at wavenumber i, and w_1 and w_2 define the spectral range. The resulting image represents a qualitative map of spectral similarity between the cartilage sample and component of interest. Euclidean distance maps for multiple components (e.g.

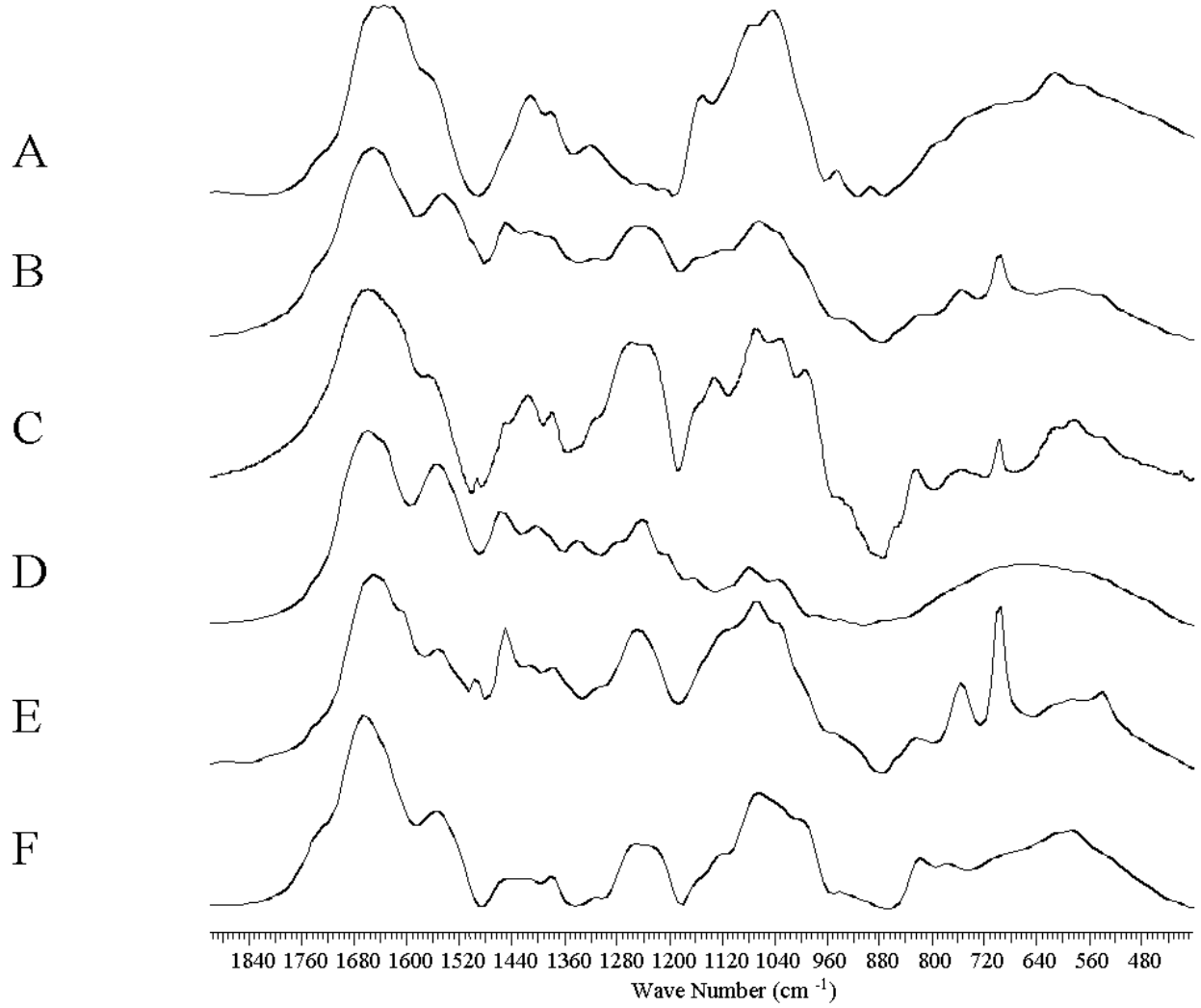

Figure 2: FTIR spectra of standards: A) Hyaluronic Acid B) Decorin C) Chondroitin-6-Sulphate D) Type II Collagen E) Biglycan F) Aggrecan. Notable absorbance peaks for collagen include the Amide I (1658 cm^{-1}), Amide II (1550 cm^{-1}), Amide III (1242 cm^{-1}), while the proteoglycans exhibit absorbance peaks for the Amide I stretch (1652 cm^{-1}), Amide II and N-H bend (1559 cm^{-1}), Sulphate stretch (1243 cm^{-1}) and the carbohydrate ring vibrations (926-1166 cm^{-1})

collagen and CS6) were superimposed to create a colour image where each component's distance is represented by a primary colour (red or blue). Common regions of spectral similarity combined to give a secondary colour (magenta), while low intensity or black colour corresponded to mutually dissimilar regions.

A quantitative assessment of component concentration was performed using PLS. The relative concentration of matrix components was determined by assuming that the sample cartilage spectra represent a linear combination of their collagen and proteoglycan components. For each dataset a partial least squares model is constructed from the reference spectra and fit on a pixel by pixel basis to give relative concentration maps for each component. In this study, the model was limited to collagen and CS6 as the primary components of the extracellular matrix. Regions of interest were identified manually to calculate the relative mean component concentrations for each sample. Additionally, the territorial and inter-territorial matrix sites were manually segmented to investigate the degree of extracellular heterogeneity.

Statistical analysis

FTIRI PLS data are reported as mean (of some number of pixels within the section) ± standard deviation. Statistical comparisons with histological results were done using a non-parametric Spearman correlation and Student *t*-test ($p < 0.05$ was considered significant).

Results

Radiological and histological grading

Pre-operative radiographs confirmed moderate to severe joint space narrowing and/or the presence of osteophytes in all subjects. All four knee replacement patients were diagnosed with Kellgren-Lawrence grade III OA while the single hip replacement patient was found to be grade IV. Histological sections of cartilage at lesion sites were found to have a mean Mankin score (out of 12) of 8.8 ± 2.2 while adjacent tissue was 4.0 ± 0.8 and control tissue was 4.3 ± 1.3. Significant differences ($p < 0.01$, $p < 0.05$) were found for lesion *vs.* adjacent and control tissue respectively. No

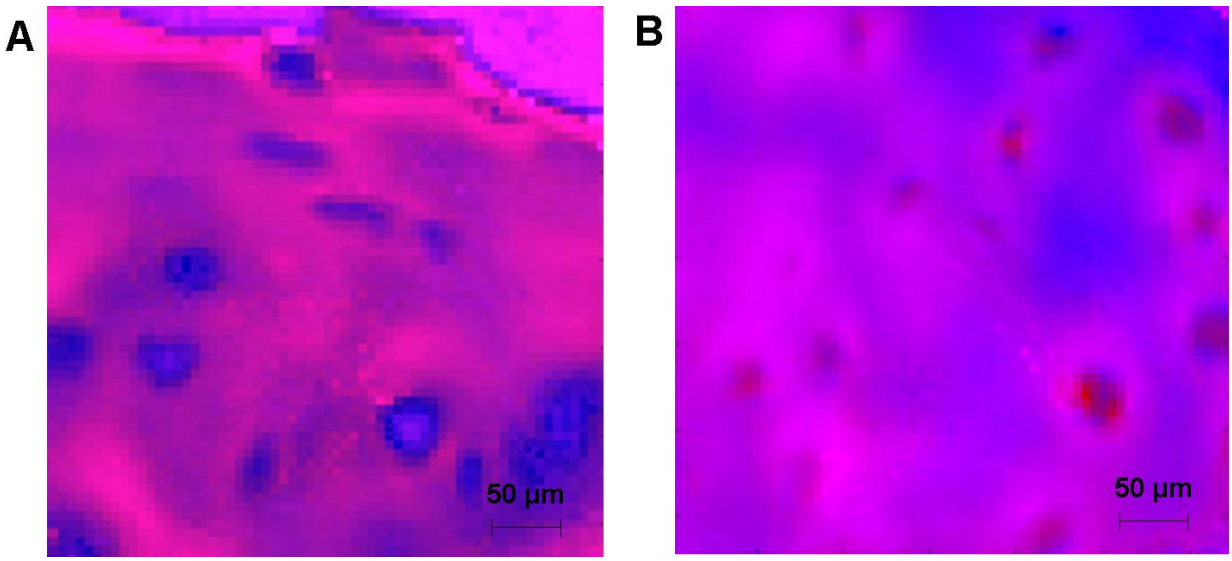

Figure 3: Representative red-blue composite images of Euclidean distance maps for CS6 and collagen in the superficial (A) and intermediate (B) layers from a healthy sample (control). In these images blue represents collagen, red represents CS6 and magenta represents both collagen and CS6. (Independent colour scale)

significant difference in Mankin score was found between the adjacent and control tissue groups. One outlier sample with a score greater than two standard deviations difference from the mean was removed.

Pure components results and spectra analysis

The FTIR spectra for type-II collagen, CS6, biglycan, decorin and aggrecan are shown in Figure 2. The characteristic features for collagen were compared with peak assignments derived from literature (Huc and Sanejouand, 1968; Lazarev *et al*., 1985). The collagen spectrum exhibits typical features of a protein spectrum with absorbance band at 1649 cm^{-1} (amide I), 1545 cm^{-1} (amide II) and at 1250 cm^{-1} (amide III). The main features of the CS6 spectra arise from sugar groups ranging from 1000 to 1200 cm^{-1}, sulphate (1240 cm^{-1}) and carboxylate absorbance bands (1610 cm^{-1}, 1411 cm^{-1}). These data were consistent with prior published spectra for CS6 (Orr, 1954). There is considerable overlap in the absorbance bands for methylene (1480 cm^{-1}), methyl (1375 cm^{-1}), amide I and II between collagen and CS6.

Qualitative analysis

Euclidean distance analysis was performed on all FTIRI datasets using the reference type-II collagen and CS6 spectra. Representative red-blue composite distance maps for CS6 and type-II collagen are shown in Figure 3. CS6 (red) was seen primarily in the matrix adjacent to the cells (the pericellular space). In contrast, the interterritorial space appeared blue indicating a strong spectral similarity with collagen. This was especially evident in maps of the collagen-rich intermediate layer. The territorial space between cells appeared magenta due to contribution of both CS6 and collagen. As with CS6, aggrecan was found to have highest spectral similarity in the pericellular space, with content in the area immediately adjacent to cells compared to the interterritorial space. High spectral similarity was found for decorin and biglycan in the superficial zone and the pericellular space with decorin primarily adjacent to the cells.

Semi-quantitative analysis

Collagen and CS6 content in the specimen

A partial least squares analysis was performed on the FTIRI datasets to extract constituent concentrations for CS6 and type-II collagen within the different layers. Combining data for all tissue samples, cartilage was found to be 38% ± 10 % collagen and 22% ± 9% CS6. From the articular surface and moving towards the deep layer relative CS6 content was found to be 19% ± 8%, 23% ± 8% and 24% ± 10% respectively.

At an individual level (see Figure 4), the CS6 PLS score difference (lesion versus adjacent tissue) was found to be significantly lower ($p < 0.0001$) in the superficial layer. The mean difference approaches 0 in the mid layer and increases again in the deep layer. No significant lesion *vs.* surrounding differences in the collagen content were found across cartilage layers.

Biochemical modifications according to histological severity of OA.

As seen in Figure 5, the CS6 concentration varied with histological degeneration as assessed by the Mankin score. Significant ($p < 0.0008$) loss was seen in the superficial layer of specimens with severe osteoarthritis (Mankin score 8-12) compared to those with mild OA (Mankin score ranging from 0-4). CS6 loss was also significant for specimens with mild compared to moderate OA ($p < 0.004$) and moderate to severe OA ($p < 0.05$). In contrast, the only significant difference in collagen content of the superficial layer was found between moderate and severe degeneration ($p < 0.05$). Using the Spearman correlation, it was confirmed that a significant loss of CS6 in the superficial layer was associated with histological severity ($R = -0.69$; $p < 0.0008$). There was also a significant correlation between collagen content in the intermediate

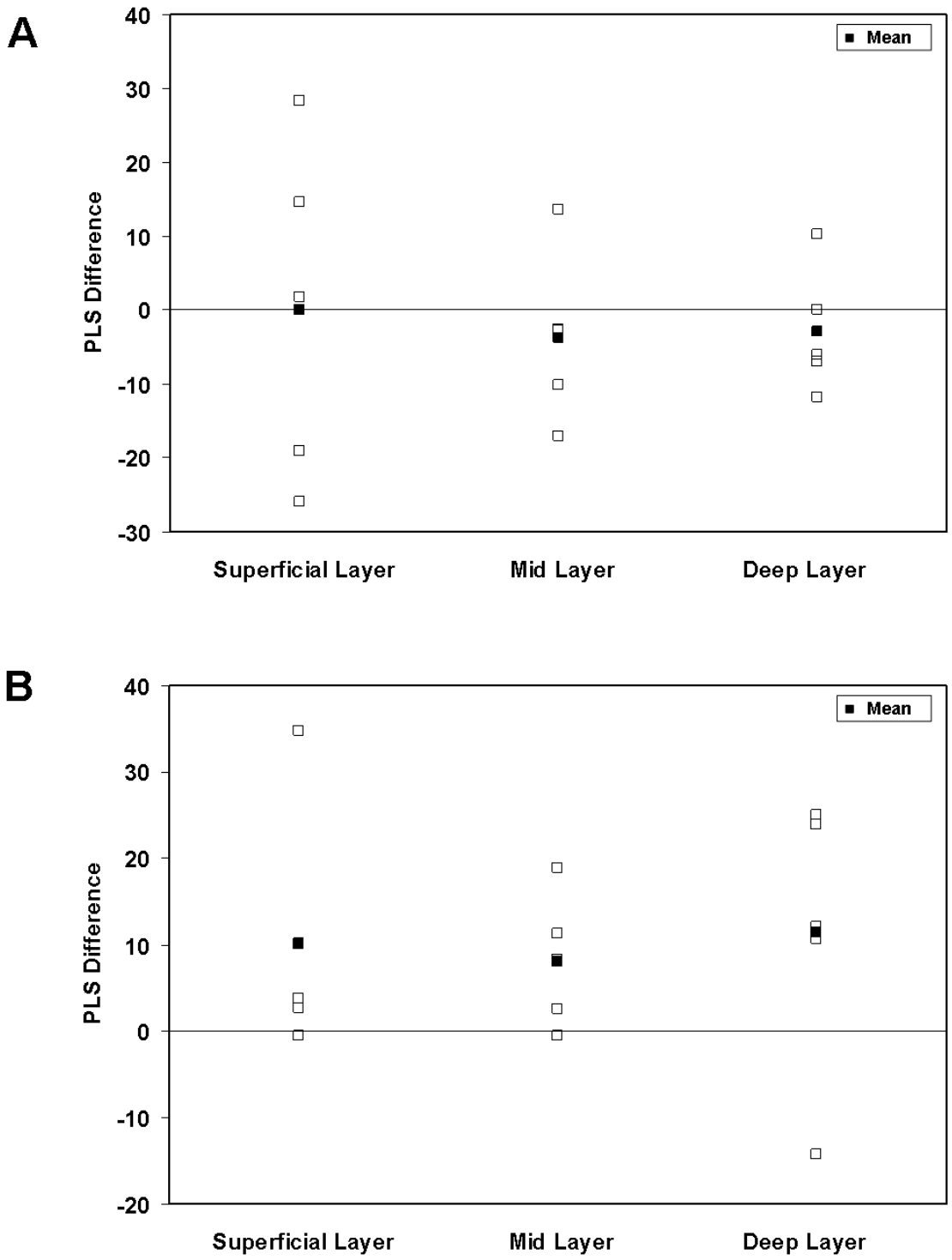

Figure 4: Difference in PLS between region adjoining the lesion and lesion in (A) CS6 and (B) collagen content in the different layers of the specimen

and superficial layer (R = 0.64, $p < 0.003$) as well as between the deep and intermediate layer (R = 0.54, $p < 0.02$). This suggests that changes in collagen distribution are consistent across cartilage layers, regardless of the OA stage.

Distribution across the matrix of collagen molecules

The pixel to pixel variation in collagen content across the section reflects the heterogeneous distribution of collagen. As shown in Figure 6, collagen was located primarily in the interterritorial matrix (TM/ITM < 1). The TM/ITM ratio for collagen did not vary in mild and moderate osteoarthritis. The regional variation across the matrix was especially marked in the superficial layer where degradation occurs in the pericellular and territorial matrix and precedes the interterritorial changes. The TM/ITM ratio for CS6 was > 1, indicating that CS6 is located primarily in the territorial matrix.

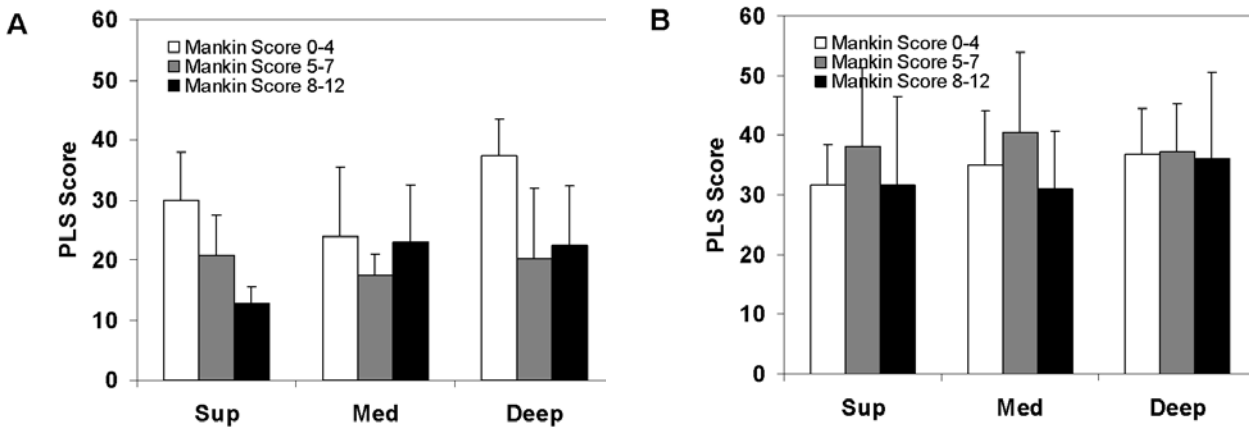

Figure 5: (A) CS6 content variation with Mankin Score in terms of the PLS score. (B) Collagen content variation with Mankin Score in terms of the PLS score. Sup: superficial; Med: intermediate; Deep Layers.

Discussion

In this paper the biochemical nature of human osteoarthritic articular cartilage was investigated using several physical and microscopic methods. Quantitative information about the distribution of the major chemical constituents of articular cartilage was evaluated with FTIRI. This marks one of the first reports on differences in collagen and proteoglycan distribution not only in different cartilage layers, but in focal lesion areas, in cartilage tissue adjoining the lesion, and in control cartilage. Specific spectral absorbance bands arising from the major components of cartilage were difficult to identify because of the significant spectral overlap for collagen, proteoglycans, and other minor matrix proteins; thus, peak ratio intensity measurements were not sufficient. Instead a multivariate analysis was used to obtain semi-quantitative measurements for type-II collagen and chondroitin 6-sulphate.

Considerable individual and inter-individual variation was found in both the distribution and content of collagen and proteoglycan underscoring the heterogeneity of the OA process as shown in previous studies (Rizkalla *et al*., 1992). Substantial variations of the major components across the different layers were also evident. Nevertheless, CS6 content is clearly lowest in the superficial layer while the highest density of collagen molecules corresponds to the tangential region just under the articular surface. These findings are in agreement with previous studies (Camacho *et al*., 2001).

At an individual level, cartilage from a focal lesion contains less CS6 compared to cartilage adjacent to the lesion highlighting the focal process of OA. These results are similar to those obtained by Squires *et al*. (2003) for early focal lesions and adjacent areas in aging cartilage. Our results fail to demonstrate an increase in CS6 content in control samples.

Using Euclidean distance collagen mapping combined with PLS analysis it was confirmed that collagen molecules were primarily located in the interterritorial matrix of osteoarthritic cartilage. The ratio of territorial to interterritorial matrix collagen increased in the intermediate and deeper layers. This suggested increased collagen deposition in the territorial matrix of the deep layer is an indication of repair (Pfander *et al*., 1999). In contrast, CS6 was mainly located in the pericellular space (TM/ITM always >1) which was consistent with histological staining. The Mankin grade is a composite score used to evaluate histological degeneration associated with osteoarthritis. It has been criticized for its complexity since it takes into account architectural features, cellular, and chemical modifications related to OA. In this study, Mankin score was well correlated to biochemical parameters determined by FTIRI. Histological correlations based on the modified Mankin score suggested that degeneration was strongly associated with CS6 loss in the superficial layer; with a loss of proteoglycan staining, especially near the articular surface. There was also evidence for collagen degradation in the superficial zone at the end stage of OA (Mankin score 8-12). We would have expected to have a lower collagen content in moderate OA than in mild OA since the collagen denaturation occurs early in the osteoarthritic process (Hollander *et al*., 1995).

Biglycan and Decorin are small proteoglycans, members of the leucin-rich repeat protein family. Biglycan is composed of a 38 kDa core protein that is substituted with 2 GAGs chains on N-terminal Ser-Gly sites (Neame *et al*., 1989; Fisher *et al*., 1991). Biglycans are found in the interterritorial matrix and in the pericellular area where they are thought to modulate morphogenesis and differentiation (Stanescu, 1990). Decorin is mainly located in the interterritorial matrix involved in the regulation of important biological functions like matrix organization, cell adhesion, migration and proliferation (Gallagher, 1989; Bock *et al*., 2001). In this study, quantification of the concentration and distribution of different proteoglycans such as decorin, biglycans, aggrecan, hyaluronic acid was difficult due to considerable overlap of the spectra. Although maps of spectral similarity based on the Euclidean distance were calculated for each of these components, it's not clear that such methods truly differentiate between the individual proteoglycans. For this reason, this paper focused on the CS6 and collagen peak features of osteoarthritic cartilage.

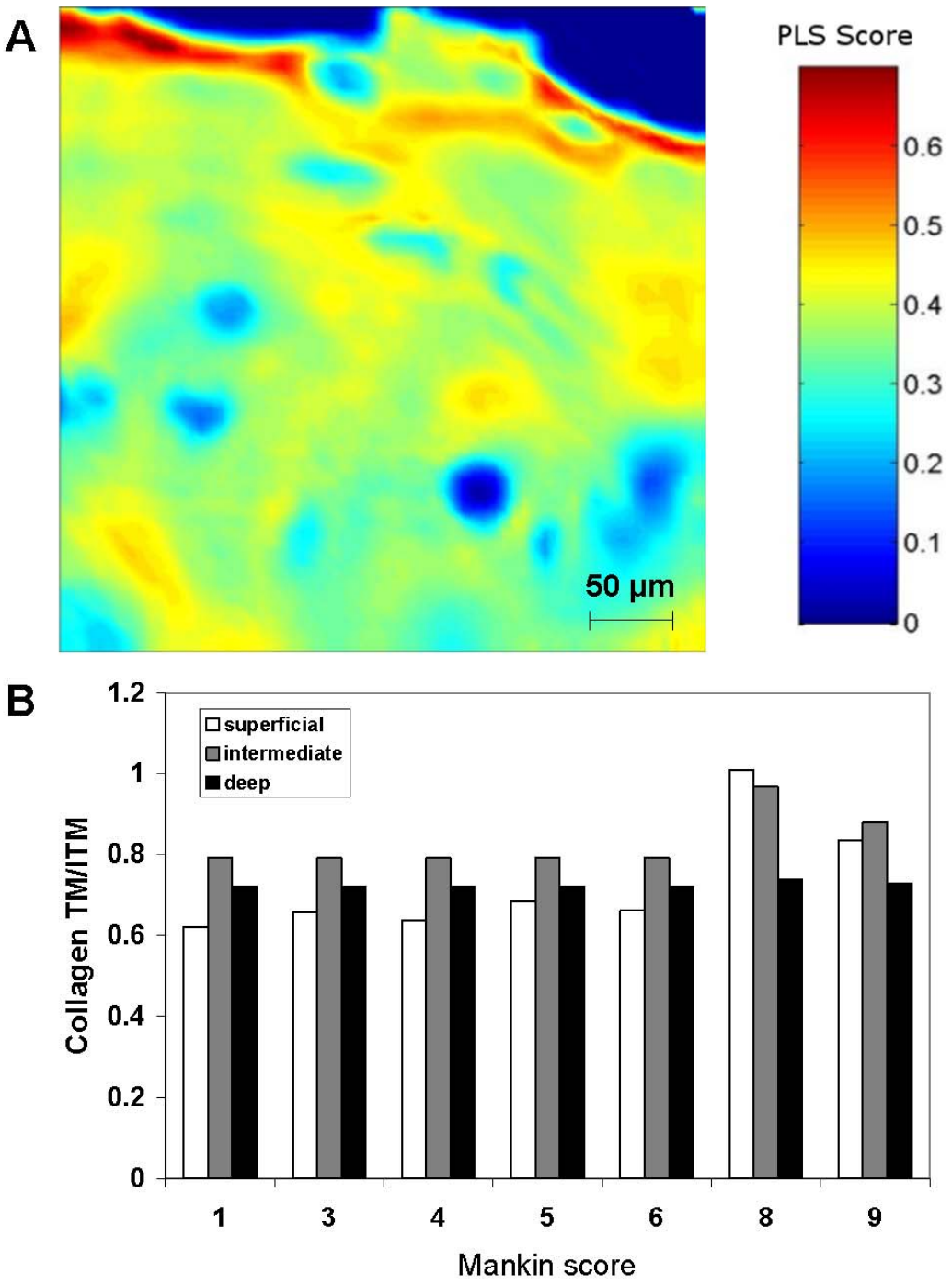

Figure 6: (A) PLS for collagen mapping displaying the matrix distribution. (B) Collagen distribution in the matrix for the different layers according to histological severity.

Lower relative concentrations of CS6 and collagen were found in this study compared to previous work with bovine nasal cartilage (Potter *et al*., 2001). This can probably be attributed to the fact that diseased human cartilage is known to contain fewer macromolecules. In this respect, it would have been interesting to include non-diseased cartilage as a true control. Moreover, the comparison between bovine and human cartilage is also difficult since there are important variations between species.

Recent studies in magnetic resonance techniques show increased relaxation time measurements in OA (David-Vaudey *et al*., 2004; Dunn *et al*., 2004) but these methods are indirect measures of cartilage biochemistry. High frequency ultrasonography was also assessed for disease progression in osteoarthritis with promising correlation for collagen content in osteoarthritic samples (Saied *et al*., 1997; Cherin *et al*., 2001). However, proteoglycan depletion is more difficult to evaluate with this technique (Pellaumail *et al*., 2002). Histology is used to quantify proteoglycan depletion using Safranin-O intensities (Camplejohn and Allard, 1988) but for advanced osteoarthritis, the reliability of staining intensity and proteoglycan content is more controversial (Rosenberg,

1971). Ultrastructural techniques, such as radio-immunoassay (Poole *et al*., 1996), are applied to study compositional changes in articular cartilage with great precision. Infrared technology provided both quantitative and qualitative analysis and allowed the quantification of many components at the same time. In this respect, FTIR combined imaging qualities and chemical information. The other advantage of this technique stems from the fact that no marker molecule was required and most importantly the morphological characteristics were preserved, allowing for a detailed account of variations in biochemical properties as a function of anatomical position. Nevertheless, limitations of the technique come from the fact that for processing, tissue sections are usually dehydrated, therefore accurate results are difficult to obtain since water is known to be extremely important in cartilage biochemistry.

In the future, it would be relevant to use FTIRI to assess the biochemical modifications in a larger population, to include normal and early stage OA, and to compare the quantitative results against biochemical bulk analysis as a gold standard. Identification of these changes is of interest to better understand the pathogenesis of osteoarthritis and prevent disease progression.

References

Bock HC, Michaeli P, Bode C, Schultz W, Kresse H, Herken R, Miosge N (2001) The small proteoglycans decorin and biglycan in human articular cartilage of late-stage osteoarthritis. Osteoarthritis Cartilage **9**: 654-663.

Boskey AL, Gadaleta S, Gundberg C, Doty SB, Ducy P, Karsenty G (1998) Fourier transform infrared microspectroscopic analysis of bones of osteocalcin-deficient mice provides insight into the function of osteocalcin. Bone **23**: 187-196.

Boskey AL, Spevak L, Paschalis E, Doty SB, McKee MD (2002) Osteopontin deficiency increases mineral content and mineral crystallinity in mouse bone. Calcif Tissue Int **71**: 145-154.

Camacho NP, Landis WJ, Boskey AL (1996) Mineral changes in a mouse model of osteogenesis imperfecta detected by Fourier transform infrared microscopy. Connect Tissue Res **35**: 259-265.

Camacho NP, Rimnac CM, Meyer RA Jr, Doty S, Boskey AL (1995) Effect of abnormal mineralization on the mechanical behavior of X-linked hypophosphatemic mice femora. Bone **17**: 271-278.

Camacho NP, West P, Torzilli PA, Mendelsohn R (2001) FTIR microscopic imaging of collagen and proteoglycan in bovine cartilage. Biopolymers **62**: 1-8.

Camplejohn KL, Allard SA (1988) Limitations of safranin 'O' staining in proteoglycan-depleted cartilage demonstrated with monoclonal antibodies. Histochemistry **89**: 185-188.

Cassella JP, Barrie PJ, Garrington N, Ali SY (2000) A fourier transform infrared spectroscopic and solid-state NMR study of bone mineral in osteogenesis imperfecta. J Bone Miner Metab **18**: 291-296.

Cherin E, Saied A, Pellaumail B, Loeuille D, Laugier P, Gillet P, Netter P, Berger G (2001) Assessment of rat articular cartilage maturation using 50-MHz quantitative ultrasonography. Osteoarthritis Cartilage **9**: 178-186.

Choo LP, Wetzel DL, Halliday WC, Jackson M, LeVine SM, Mantsch HH (1996) *In situ* characterization of beta-amyloid in Alzheimer's diseased tissue by synchrotron Fourier transform infrared microspectroscopy. Biophys J **71**: 1672-1679.

Cooper EA, Knutson K (1995) Fourier transform infrared spectroscopy investigations of protein structure. Pharm Biotechnol **7**: 101-143.

David-Vaudey E, Ghosh S, Ries M, Majumdar S (2004) T2 relaxation time measurements in osteoarthritis. Magn Reson Imaging **22**: 673-682.

Dunn TC, Lu Y, Jin H, Ries MD, Majumdar S (2004) T2 relaxation time of cartilage at MR imaging: comparison with severity of knee osteoarthritis. Radiology **232**: 592-598.

Fisher LW, Heegaard AM, Vetter U, Vogel W, Just W, Termine JD, Young MF (1991) Human biglycan gene. Putative promoter, intron-exon junctions, and chromosomal localization. J Biol Chem **266**: 14371-14377.

Gallagher JT (1989) The extended family of proteoglycans: social residents of the pericellular zone. Curr Opin Cell Biol **1**: 1201-1218.

Gao T, Feng J, Ci Y (1999) Human breast carcinomal tissues display distinctive FTIR spectra: implication for the histological characterization of carcinomas. Anal Cell Pathol **18**: 87-93.

Hollander AP, Pidoux I, Reiner A, Rorabeck C, Bourne R, Poole AR (1995) Damage to type II collagen in aging and osteoarthritis starts at the articular surface, originates around chondrocytes, and extends into the cartilage with progressive degeneration. J Clin Invest **96**: 2859-2869.

Huc A, Sanejouand J (1968) Study of the infra-red spectrum of acid-soluble collagen. Biochim Biophys Acta **154**: 408-410.

Hyllested JL, Veje K, Ostergaard K (2002) Histochemical studies of the extracellular matrix of human articular cartilage-a review. Osteoarthritis Cartilage **10**: 333-343.

Jackson M, Mantsch HH (1995) The use and misuse of FTIR spectroscopy in the determination of protein structure. Crit Rev Biochem Mol Biol **30**: 95-120.

Kellgren JH, Lawrence JS (1957) Radiological assessment of osteo-arthrosis. Ann Rheum Dis **16**: 494-502.

Kidder LH, Kalasinsky VF, Luke JL, Levin IW, Lewis EN (1997) Visualization of silicone gel in human breast tissue using new infrared imaging spectroscopy. Nat Med **3**: 235-237.

Lasch P, Naumann D (1998) FT-IR microspectroscopic imaging of human carcinoma thin sections based on pattern recognition techniques. Cell Mol Biol (Noisy-le-grand) **44**: 189-202.

Lazarev YA, Grishkovsky BA, Khromova TB (1985) Amide I band of IR spectrum and structure of collagen and related polypeptides. Biopolymers **24**: 1449-1478.

Ma H, Huang Y, Lei H (2001) New applications of

FTIR micro-spectroscopy in the field of forensic science. Guang Pu Xue Yu Guang Pu Fen Xi **21**: 468-471.

Mankin HJ, Johnson ME, Lippiello L (1981) Biochemical and metabolic abnormalities in articular cartilage from osteoarthritic human hips. III. Distribution and metabolism of amino sugar-containing macromolecules. J Bone Joint Surg Am **63**: 131-139.

Neame PJ, Choi HU, Rosenberg LC (1989) The primary structure of the core protein of the small, leucine-rich proteoglycan (PG I) from bovine articular cartilage. J Biol Chem **264**: 8653-8661.

Orr SF (1954) Infra-red spectroscopic studies of some polysaccharides. Biochim Biophys Acta **14**: 173-181.

Paschalis EP, Betts F, DiCarlo E, Mendelsohn R, Boskey AL (1997) FTIR microspectroscopic analysis of human iliac crest biopsies from untreated osteoporotic bone. Calcif Tissue Int **61**: 487-492.

Paschalis EP, Jacenko O, Olsen B, deCrombrugghe B, Boskey AL (1996) The role of type X collagen in endochondral ossification as deduced by Fourier transform infrared microscopy analysis. Connect Tissue Res **35**: 371-377.

Pellaumail B, Watrin A, Loeuille D, Netter P, Berger G, Laugier P, Saied A (2002) Effect of articular cartilage proteoglycan depletion on high frequency ultrasound backscatter. Osteoarthritis Cartilage **10**: 535-541.

Pfander D, Rahmanzadeh R, Scheller EE (1999) Presence and distribution of collagen II, collagen I, fibronectin, and tenascin in rabbit normal and osteoarthritic cartilage. J Rheumatol **26**: 386-394.

Poole AR, Rosenberg LC, Reiner A, Ionescu M, Bogoch E, Roughley PJ (1996) Contents and distributions of the proteoglycans decorin and biglycan in normal and osteoarthritic human articular cartilage. J Orthop Res **14**: 681-689.

Potter K, Kidder LH, Levin IW, Lewis EN, Spencer RG (2001) Imaging of collagen and proteoglycan in cartilage sections using Fourier transform infrared spectral imaging. Arthritis Rheum **44**: 846-855.

Realini M, Rampazzi L, Colombo C, Toniolo L (2001) Atypical coloration of plaster in renaissance frescoes. Ann Chim **91**: 795-801.

Rizkalla G, Reiner A, Bogoch E, Poole AR (1992) Studies of the articular cartilage proteoglycan aggrecan in health and osteoarthritis. Evidence for molecular heterogeneity and extensive molecular changes in disease. J Clin Invest **90**: 2268-2277.

Rosenberg L (1971) Chemical basis for the histological use of safranin O in the study of articular cartilage. J Bone Joint Surg Am **53**: 69-82.

Saied A, Cherin E, Gaucher H, Laugier P, Gillet P, Floquet J, Netter P, Berger G (1997) Assessment of articular cartilage and subchondral bone: subtle and progressive changes in experimental osteoarthritis using 50 MHz echography *in vitro*. J Bone Miner Res **12**: 1378-1386.

Squires GR, Okouneff S, Ionescu M, Poole AR (2003) The pathobiology of focal lesion development in aging human articular cartilage and molecular matrix changes characteristic of osteoarthritis. Arthritis Rheum **48**: 1261-1270.

Stanescu V (1990) The small proteoglycans of cartilage matrix. Semin Arthritis Rheum **20**(3 Suppl 1): 51-64.

Discussion with Reviewers

D. Jones: This is an interesting and potentially powerful application of the technique, though the statement that it is new (in the first sentence) is subjective. In Boskey's work, due to the poor penetration of the IR (due to water), the depth of analysis is very low and the sections used were very thin. What is the maximum depth of field of this analysis?

Authors: That is correct that the technique, like Boskey's is limited to very thin sections. The maximum thickness in our experiment was 7 microns. According to Michael Jackson (Handbook of Vibrational spectroscopy p. 3378), samples should be normally prepared as thin sections (5-20 microns) from fresh frozen tissue without any fixatives or embedding. For infrared transmission applications in such materials (i.e. soft tissue) this is pretty much limited to 10 microns.